Characterization of a SDR Front-End Receiver With Multisine Excitations

Pedro Cruz[#1], Nuno Borges Carvalho[#2]

[#]*Instituto de Telecomunicações, Universidade de Aveiro*
Campus Universitário de Santiago, Aveiro, Portugal
[1]pcruz@av.it.pt [2]nbcarvalho@ua.pt

***Abstract*— The paper presents an evaluation of the nonlinear distortion sources in software-defined radio front-ends, based on band-pass sampling receivers. These nonlinear mechanisms are for the first time modelled for SDR receivers.**

This behavioral model is a combination of Volterra Series and large signal operation represented by a clipping function followed by a black-box representing the quantization and sampling schemes of the ADC. The model is then validated by using several multisine signals with different signal statistics.

The obtained results validate the proposed behavioral model for SDR wireless system design.

I. Introduction

THIS paper will evaluate the nonlinear phenomena in specific software-defined radio (SDR) receivers that are based on band-pass sampling configurations. This will be complemented by studying their impact on the wireless communication receiving chain and by proposing a simple behavioral model that will allow wireless system design engineers to efficiently simulate signal degradation due to the nonlinear distortion in the SDR receiver.

The concept of SDR first appeared with the work of Mitola [1] in 1995. In this work, he purposed to create a radio that is fully adaptable by software, enabling the radio to adjust to several communication scenarios automatically. The concept is presented in Fig. 1.

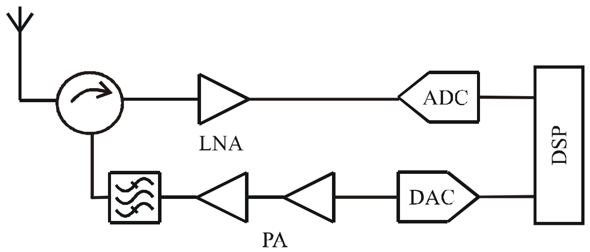

Fig. 1 – Common implementation of the software-defined radio concept from [1].

The ideal software-defined radio will adapt itself to the transmission scenario by gathering information about all of the signals that are present in the air interface.

The motivation behind this concept is not only the high flexibility to adapt the front-end to simultaneously operate with any modulation, channel bandwidth, or carrier frequency, but also the possible cost savings that integrating in full digital technology could yield.

Moreover a well-designed architecture of a multi-band multi-mode receiver should optimally share the available hardware resources and make use of tunable and software programmable devices.

These facts impose that these types of radios should be wideband, and have high dynamic range simultaneously. The bandwidth is mainly controlled by the sampling and hold circuit restrictions, while the high dynamic range is controlled by the receiving noise, imposed by the LNA and filtering capabilities, and by the high power that the receiver can accept. This high power necessity is mainly associated to the high values of PAPR of nowadays wireless standard radios, and by the possible existence of out of band interferes.

In this paper we first give a short analysis of the nonlinear distortion sources of an SDR front-end based on band-pass sampling receiver that was presented in [2], which is the used architecture for the rest of the paper. Also, in Section II, a reviewed behavioral model that combines all the sources of nonlinear distortion in the band-pass sampling receiver will be presented.

Moreover, the extraction procedure of this model will also be described in Section III. In contrast to the Volterra-series-based procedure for ADC distortion modeling presented in [3], here we account for small-signal as well as large-signal operation.

In Section IV, the behavioral model will be used when the SDR receiver front end is excited by modulated signals having high PAPR, using several multisines with different statistical patterns.

Finally, some conclusions will be drawn taking into account the obtained results.

II. SDR Front-End Receiver Nonlinearities

As explained in [2, 4], the fundamental concept of the band-pass sampling receiver is to design a receiver with a reduced number of components taking advantage of the digital signal processing capabilities to produce the required performance.

Taking into account this type of receiver we will review the main sources of nonlinear distortion generated by its components, in which are include a band-pass filter, a low-noise amplifier (LNA) and an analog-to-digital converter (ADC). The main idea is to develop a black-box behavioral model to characterize it.

Concerning on the filter component, if we consider a static filter made of non-semiconductor devices, then the filter can be considered linear unless some passive intermodulation, PIM [5], is measured, which we do not consider in this case. Furthermore, if the filter is built with semiconductor devices, as for example varactors, or newly materials based on ferroelectric, then some amount of nonlinear distortion can exist. Nevertheless the nonlinear distortion that is expected from these components is sufficiently reduced compared with the following ones, so a linear transfer function will be enough to represent this type of filtering.

Regarding the second component (LNA) much has been written about nonlinear distortion in such type of components, for instance in [6].

In small-signal operation, nonlinear behavior is often approximated by a simple polynomial, for instance a Taylor series may be used if the transistor can be considered memoryless. For systems with memory, a Volterra-series analysis can be considered, since it will incorporate dynamic, baseband effects and thus will approximate more conveniently the behavior of the LNA small signal distortion.

In large-signal operation, the transistor starts to clip the output signal due to the fact that it will compress and saturate and it can be approximated by a large-signal transfer function, often by a describing function approach [6, 7].

The last analog component in this receiver chain is the ADC that is also responsible for creating nonlinear distortion.

One of the sources of nonlinear distortion in an ADC is the nonlinearity of its transfer function that can be responsible for missing bits, and subsequent integral nonlinearity and differential nonlinearity (INL/DNL). This nonlinear behaviour can be efficiently modelled by using a polynomial function (followed by an ideal quantizer), and thus is similar to the small-signal distortion behaviour of the LNA.

Another source of nonlinear distortion common to ADCs is related to the maximum voltage that the ADC can digitize without clipping. This distortion is amplitude dependent and is of great importance in many new wireless communication systems due to the high PAPR of their signals. This form of clipping is what is called hard clipping and is imposed by a transfer function that limits the output signal right after the input signal traverses a certain threshold.

The remaining source of nonlinear distortion in ADCs is the well-known quantization process. This highly nonlinear operation also gives rise to a high value of interference called quantization noise. Quantization phenomena changes a sine wave from a smooth function to a staircase signal and due to this nonlinear effect, the output signal is composed of a large number of nonlinear distortion products.

So, in order to be able to describe most of the previous sources of nonlinear distortion, a band-pass behavioural model will be described that represents the non-ideal behaviour of the SDR front-end architecture, Fig. 2.

The first block of the model that we will use, is the small-signal model to represent the nonlinearity of the LNA and of the ADC transfer functions. This is represented by a Volterra series approximation.

The large-signal operation of the low-noise amplifier is represented by a clipping function that could be described by a hyperbolic tangent or any other limiting function [8]. The signal is then ideally sampled and ideally quantized, in which the ADC full-scale define the quantizer boundaries.

We consider that the nonlinear behaviour due to the non-monotonic performance of the ADC will be included into the Volterra series. Because we are measuring the overall system from the output terminals, information on individual nonlinearities inside the system is not available and we are free to group them as we like.

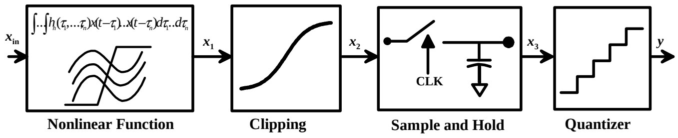

Fig. 2 – Proposed behavioral model of the SDR front-end.

Looking at the previous model we can clearly identify each block. Thus,

$$x_1(t)=\sum_{n=0}^{\infty}\int_{-\infty}^{\infty}\cdots\int_{-\infty}^{\infty} h_n(\tau_1,\cdots,\tau_n)\,x_{in}(t-\tau_1)\cdots x_{in}(t-\tau_n)\,d\tau_1\cdots d\tau_n\,, \quad (1)$$

$$x_2(t)=k.\tanh[\alpha.x_1(t)]\,, \quad (2)$$

$$x_3[n]\equiv x_3(nT)=\sum_{n=-\infty}^{+\infty}x(t).\delta(t-nT)\,, \quad (3)$$

$$y[n]=Quant(x_3[n])\,, \quad (4)$$

where $x_{in}(t)$ is the input signal waveform, $h_n(\tau_1,\ldots,\tau_n)$ is the n^{th} order Volterra kernel, *tanh*[.] symbolize the hyperbolic tangent in which k and α are adjusting amplitude values, $\delta(t)$ denotes the Dirac delta function, and *Quant*(.) represents the quantization process.

III. Model Parameter Extraction of a SDR Receiver

In order to demonstrate the validity of the proposed behavioral model a band-pass sampling receiver, similar to the one described in [2], was implemented. Our receiver approach to be modeled does not include the digital front-end which follows the ADC (digital signal processing), nor the required wideband receiving antennas.

So, we use a fixed band-pass filter to select the 5^{th} Nyquist zone, and avoid aliasing of other undesired signals, followed by a commercially wideband (0.5 – 1000MHz) LNA which has a 1dB compression point of +9dBm, an approximated gain of 24dB, and a noise figure near to 6dB, and finally a commercially 12-bit pipeline ADC that has a linear input range of +11dBm with a analog input bandwidth of 750MHz. To finish, a clock frequency of 100MHz was applied because some limitations in the instrumentation used.

A model is only good if the extraction and model development procedures are quite simple and efficient. In this model, the polynomial (Volterra) parameters can be extracted by using small-signal measurements. For the third-order nonlinear descriptor, we will use the zone of the third-harmonic output where the distortion power rises at three decibels per decibel. The compression of the nonlinear distortion, and the fundamental signal power, will define the parameters of the hyperbolic tangent or other clipping function. Finally, the quantization and sampling block is imposed by the ADC used in the SDR front-end.

Then, the behavioral model parameter extraction was made using the set-up described in [9].

In order to extract the proposed model, a one-tone signal centered in the 5^{th} Nyquist zone, was used as the excitation and the measured results are shown in Fig. 3.

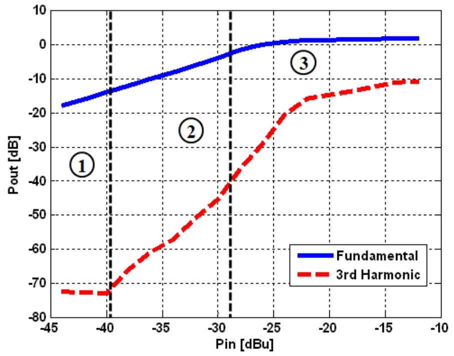

Fig. 3 – One-tone measurements for the SDR front-end receiver.

In Fig. 3, three different zones may be identified. The first zone is eliminated for parameter extraction since the harmonics that we seek are lower than the measured noise level. From the second zone, where the third-harmonic distortion rises at three decibels per decibel of input power, the third-order coefficient is extracted. Finally, the value that will be used to select the clipping breakpoint is extracted from the third zone, where the fundamental signal is near its 1dB compression point. To model large signal operation, we used a hyperbolic tangent as the clipping function, since the small signal to large signal transition is smooth.

This extraction procedure allows us to have a first estimate of the coefficients and then a least-square optimization algorithm is used to minimize the difference between measured and simulated results for the model based on the one-tone extraction.

Throughout additional experiments, we observed that our SDR front end, behaved as a memoryless system, since the coefficients did not change significantly with frequency.

In order to confirm that our model can describe the behavior of an SDR front end under modulated-signal excitations, we carried out measurements when a two-tone signal, centered in the 5^{th} Nyquist zone, was applied to the input, and compared the output values with our modeled results.

Figure 4 presents the obtained results for the output fundamental and the third-order IMD values. Good agreement can be seen between the measurements and the simulations. The observable difference between measured and simulated third-harmonic results at low input-power levels is due to the noise floor of the measurement set-up used.

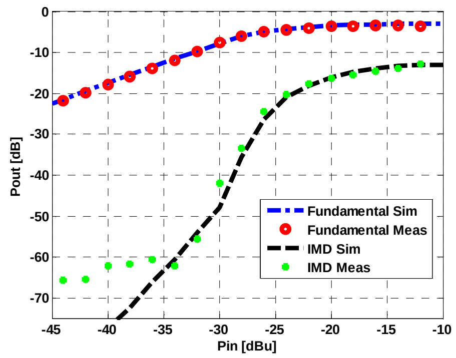

Fig. 4 – Two-tone measurements and simulations for the SDR front-end receiver.

IV. Validation of the Behavioral Model with Multisines

We use the SDR front-end receiver described in the previous section to conduct the validation of the model, using several amplitude/phase arrangements for the frequency components of the multisines, which mimic different time-domain-signal statistics and thus PAPR [10].

In this case, we used several multisines of 100 tones with a total occupied bandwidth of 1MHz. Table 1 presents the different values of PAPR for each multisine arrangement.

Table 1: PAPR for each multisine excitation.

Signal Type	**PAPR [dB]**
Uniform	2.1266
Normal	8.5184
Constant Phase	20.0000

Figure 5 presents the measured statistics for each multisine arrangement. The *Constant Phase* arrangement is the one where the relative phase difference is 0º between the tones. This yields a large value of 20dB PAPR. As can be seen from Fig. 5 and Table 1, the PAPR varies significantly with the engineered statistics of the multisine.

Figure 6 presents the measured and simulated results in which are captured the fundamental power and adjacent channel power (ACP), arising from nonlinear distortion, for each multisine excitation.

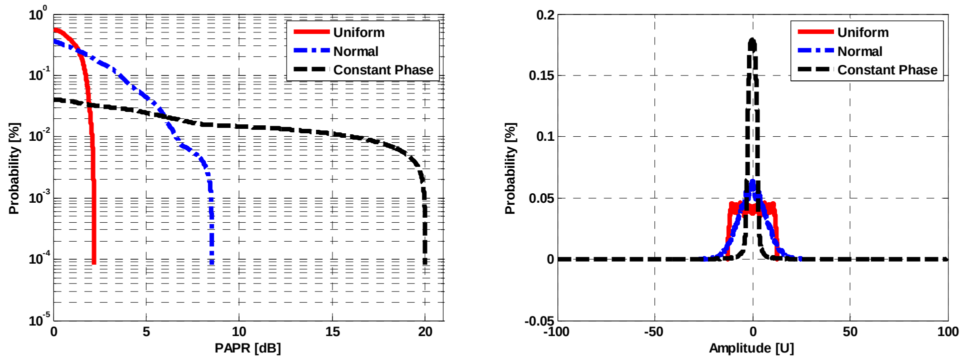

(a) (b)

Fig. 5 – Measured statistics for each multisine signal: (a) CCDF and (b) PDF.

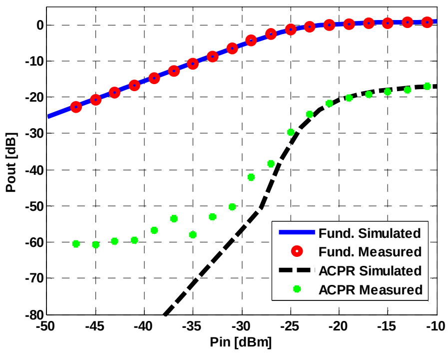

(a)

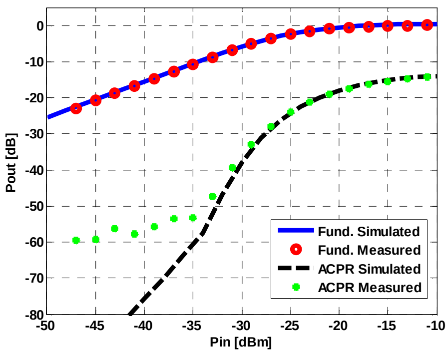

(b)

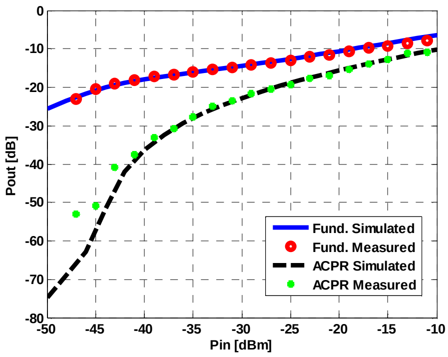

(c)

Fig. 6 – Measured and simulated results for different multisine signal statistics, (a) Uniform, (b) Normal and (c) Constant Phase.

As can be seen from the figures shown, the signal with constant-phase statistics deviates from linearity at a much lower input power level than for the other cases since the PAPR of that signal is extremely high and so clipping occurs at a relatively low input level. As well, the adjacent channel power is significantly higher for the constant phase case than for the others.

Under small-signal excitation the SDR front end is mainly ruled by quantization noise in the simulations and by instrumentation noise in the measurements.

The distortion starts then to rise for medium-signal excursions at three decibels per decibel of input power. At high input power levels, it compresses to a saturated value.

The good match between the simulations and the measurements, shown in the figures, indicates the viability of our model for nonlinear description of an SDR front-end receiver based on a band-pass sampling configuration.

V. Conclusions

We presented a short description of nonlinear distortion mechanisms in Software Defined Radio front-end receivers. We first present a reviewed model for the SDR front-end that accounts for most of the nonlinear distortion sources, mainly created by the two components: the LNA and the ADC.

It was seen that the nonlinear distortion can be a concern in systems developed for high PAPR signal handling. In that respect a behavioral model was also developed for the SDR nonlinear distortion characterization.

The performance of this model was compared to measurements of two-tone and multisines. The good agreement between the model and the measurements confirm that our model represents well the main observed characteristics. This type of model could be expanded to include additional distortion mechanisms as they are identified, for instance the nonlinearity of solid-state switches [11].

Modeling these sources of nonlinearity may be important in the design of multi-mode handsets, where very weak sources of intermodulation distortion can have an impact on successful reception of a desired signal.

References

[1] J. Mitola, “The Software Radio Architecture,” *IEEE Communications Magazine*, vol. 33, no. 5, pp. 26-38, May 1995.

[2] P. Cruz, and N.B. Carvalho, “Multi-Mode Receiver for Software Defined Radio,” *2nd Congress of Portuguese Committee of URSI*, Lisbon, pp. *tbd.*, November 2008.

[3] N. Bjorsell, P. Suchánek, P. Handel, and D. Ronnow, “Measuring Volterra kernels of analog-to-digital converters using a stepped three-tone scan,” *IEEE Trans. Instrum. Meas.*, vol. 57, no. 4, pp. 666-671, April 2008.

[4] D. Akos, M. Stockmaster, J. Tsui, and J. Caschera, “Direct bandpass sampling of multiple distinct RF signals,” *IEEE Trans. on Communications*, vol. 47, no. 7, pp. 983 – 988, 1999.

[5] P.L. Lui, “Passive Intermodulation Interference in Communications Systems,” *Electronics & Communication Engineering Journal*, June 1990.

[6] P. Wambacq, Willy M. C. Sansen, “Distortion Analysis of Analog Integrated Circuits,” *The Springer International Series in Engineering and Computer Science*, 1998.

[7] J.C. Pedro and N.B. Carvalho, *Intermodulation Distortion in Microwave and Wireless Systems and Circuits*, Artech House, London, 2003.

[8] P. Arpaia, P. Daponte, and S. Rapuano, “A State of the Art in ADC Modeling,” *Comput. Standards Interfaces*, vol. 26, pp. 31–42, 2003.

[9] P. Cruz, N.B. Carvalho, K.A. Remley, and K. Gard, “Mixed Analog-Digital Instrumentation for Software Defined Radio Characterization,” *IEEE Intl. Microwave Symp. Dig.*, Atlanta, GA, pp. *tbd.*, June 2008.

[10] P. Cruz, N.B. Carvalho, and K.A. Remley, “Evaluation of Nonlinear Distortion in ADCs Using Multisines,” *IEEE Intl. Microwave Symp. Dig.*, Atlanta, GA, pp. *tbd.*, June 2008.

[11] T. Ranta, J. Ella, and H. Pohjonen, “Antenna Switch Linearity Requirements for GSM/WCDMA Mobile Phone Front-Ends,” *European Conf. on Wireless Tech. Dig.*, Paris, pp. 23-26, Oct. 2005.